IOP Conf. Series: Materials Science and Engineering **402** (2018) 012164 doi:10.1088/1757-899X/402/1/012164

Need of different flapping styles for different flight phases of a flapping wing vehicle: A preliminary analysis

K Allwyn[*1] and L R Ganapathy Subramanian[2]

Department of Aerospace Engineering, SRM Institute of Science and Technology, Chennai, Tamil Nadu, India.

*corresponding author: allwyn.k@ktr.srmuniv.ac.in

Abstract. Flapping wing vehicles ranging from a large bird sized model to a tiny insect-sized model were made successfully. Still, there is a lot of scope for further research, since their natural counterparts outperform them in most of the flight aspects. The fact that the natural flyers change their flapping style for different flight phases is taken for investigation. Aerodynamic forces at a wing section are analyzed using the general blade-element approach. Using vector mechanics, contributions of the sectional lift and drag forces to the thrust, lift and side force of the vehicle are derived and non-dimensionalized. All the three were in terms of four non-dimensional parameters - the sectional lift to drag ratio, advance ratio, stroke plane orientation and instantaneous flapping angle. The variations of the three force components with the four non-dimensional parameters were plotted. Flapping style with minimized side force and maximized the thrust and lift production is considered as that of efficient flying. The results demand that the stroke plane orientation, speed and amplitude of flapping should be varied for different phases of flight for efficient flying.

1. Introduction

The research on flapping flight exists even since the prehistoric age. However, the pursuit of making a bird-like or insect-like aerial vehicle intensified in the recent few decades. Recently, extreme-agile UAVs are required in different fields like scientific research, cinematography and military. The inability of the fixed wing and rotorcraft flight technology to achieve such agility, which is already exhibited by natural flyers, turned the attention of researchers towards flapping wing technology.

The ongoing research in flapping wing flight technology progresses in fields of flapping mechanism[1–4], wing kinematics[5–7], aerodynamic modeling[8–11], flight dynamics and control[12]. The aerodynamic and flight dynamic findings are useful only if the flapping mechanism performs an optimized wing kinematics.

Optimization of wing kinematics for aerodynamic performance has been attempted using methods like calculus of variation[13], gradient-based and global optimization techniques[14] applied with appropriate aerodynamic models. They were done with a specific flight phase – hovering or forward flight – taken into consideration. However, the transition of flight from takeoff to a high-speed forward flight was rarely been studied.

All natural flyers exhibit a variation in the flapping style (flapping kinematics) according to the flight attitude and the flight speed[7,15–20]. Even the most successful flapping wing vehicles lack this functionality[21–23]. Hence, we decided to study the importance of this flapping style variation for an effective flapping wing flight.

Flapping wing does itself the works done by a lift producing wing and a thrust producing propeller. The lift producing ability of wing increases with flight velocity. However, the thrust producing ability of propeller reduces with flight velocity(due to the limitations in increasing the flapping speed). A clever way of solving this issue may be the variation of flapping style in the course of flight. Brown[24] observed this phenomenon in a variety of birds and summarized the results.

Here, one should remember – the lift and thrust produced by a flapping wing are the components of the resultant aerodynamic force vector in the respective directions. Hence, a proper orientation of the resultant aerodynamic force will serve achieving the required lift and thrust. The blade element approach appeared to be a better choice for an analysis in this direction.

Sachs[25] discussed on lift vector tilting in a flapping wing and the corresponding aerodynamic cost (increase in induced drag). Lift vector tilting in two directions were addressed – one in the forward direction to produce thrust and another in the lateral direction of the vehicle caused due to the inclined position of the wing during flapping. The former tilt is unavoidable due to the need for thrust production. However, the latter should be minimized especially in a straight-line flight. This emphasized on an objective to minimize the side-force component of the resultant aerodynamic force in addition to the consideration on optimizing thrust and lift.

We chose a symmetrical flapping system with a full 180^{o} flapping amplitude range and a full range ($0 – 90^{o}$) stroke plane orientation, which helps in exploring all the possible combinations of thrust, lift and side-force in varying flight speeds and flight directions in the vertical inertial plane. We employed vector mechanics scheme to resolve the sectional lift and drag components in the thrust, lift and side-force directions. We obtained the non-dimensional form of the three components and found them to be dependent on four non-dimensional parameters - sectional lift to drag ratio, advance ratio, stroke plane orientation and instantaneous flapping angle. We analyzed the three force components upon the variation of the four non-dimensional parameters.

This paper proposes the necessity to change the flapping style in different flight phases and suggests an outline, how to vary the stroke plane orientation, speed and amplitude of flapping for efficient flying.

2. Materials and methods

A simple blade element approach is adopted to investigate the resultant aerodynamic force in a wing section. Using vector mechanics, the contributions of the resultant aerodynamic force in the flight direction *x*, lateral direction *y* and the normal direction *z* are derived from the lift and drag produced by the wing section airfoil.

2.1. Assumptions and definitions

A right-handed stability axis coordinate system (compatible with vector mechanics) with the origin fixed to the wing pivot is used (figure 1). The x-axis is aligned with the flight direction.

The movement of the wing is represented by the radius vector **r**. The instantaneous position of the wing in the stroke plane is determined by the angular displacement θ and the instantaneous angular velocity is denoted by $\dot{\theta}$. The movement of the radius vector is confined to a stroke plane. Out-of-plane motions are not considered in this preliminary analysis to simplify the methodology. The orientation of the stroke plane from the flight frontal plane is given by γ.

The flapping of the wing produces a lift $\mathbf{L}'$ and drag $\mathbf{D}'$ at a wing airfoil section located at a distance *r* from the origin. Only high lift producing down-stroke of flapping is considered.

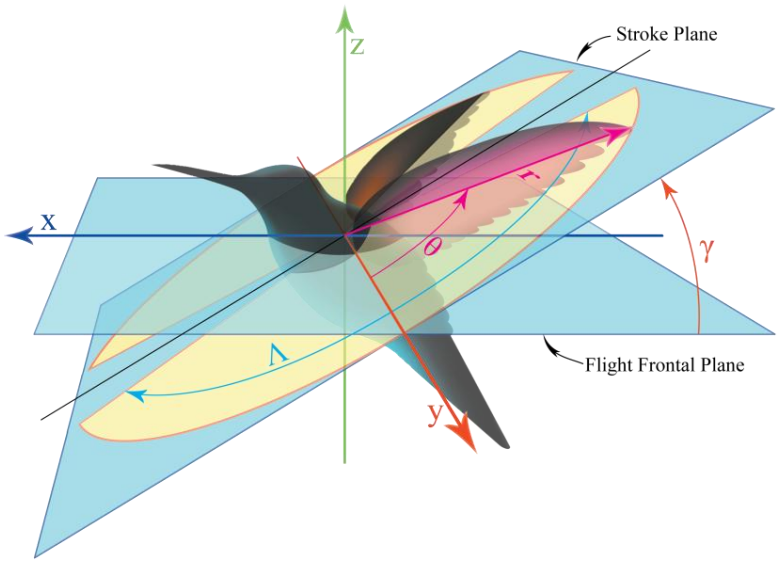

Figure 1. Right-handed stability axis system with origin fixed to the wing pivot.

2.2. Deriving the Contributions of Sectional Resultant Aerodynamic Force to Thrust, Side Force and Lift of the Vehicle

The components of the resultant aerodynamic force in the *x*, *y* and *z* directions contribute to thrust, side force and lift of the vehicle respectively.

From the basic definitions of lift and drag, it can be shown that

$$\mathbf{L}' = \tfrac{1}{2}\rho V_a{}^2 c C_l \left(\frac{\mathbf{r}\times\mathbf{V}_a}{|\mathbf{r}\times\mathbf{V}_a|} \right), \tag{1}$$

$$\mathbf{D}' = \frac{1}{2}\rho V_a{}^2 c C_d \hat{\mathbf{V}}_a \tag{2}$$

where, $\mathbf{V}_a$ is the air velocity seen by the wing section.

The resultant aerodynamic force $\mathbf{f}$ is the vector summation of the sectional lift $\mathbf{L}'$ and drag $\mathbf{D}'$.

$$\mathbf{f} = \mathbf{L}' + \mathbf{D}' \tag{3}$$

Now from equations (1), (2) and (3), the components of resultant aerodynamic force are obtained as

$$f_x = \frac{1}{2}\rho V_a{}^2 c \left(C_l \left(\frac{\sin\gamma}{g_b} \right) + C_d \left(\frac{-J - \cos\theta\cos\gamma}{g_a} \right) \right) \tag{4.a}$$

$$f_y = \frac{1}{2}\rho V_a{}^2 c \left(C_l \left(\frac{-J\sin\theta\sin\gamma}{g_b} \right) + C_d \left(\frac{-\sin\theta}{g_a} \right) \right) \tag{4.b}$$

$$f_z = \frac{1}{2}\rho V_a{}^2 c \left(C_l \left(\frac{\cos\gamma + J\cos\theta}{g_b} \right) + C_d \left(\frac{\cos\theta\sin\gamma}{g_a} \right) \right) \tag{4.c}$$

Where, $J = -V_\infty / (r\dot{\theta})$, the advance ratio, which is a non-dimensional parameter, used extensively in the blade element approach of propellers, and

$$g_a = \sqrt{J^2 + 2J\cos\theta\cos\gamma + 1} \tag{5}$$

$$g_b = \sqrt{J^2(\sin^2\theta\sin^2\gamma + \cos^2\theta) + 2J\cos\theta\cos\gamma + 1}\,. \tag{6}$$

2.3. Non-dimensionalizing the Force Components

To support a generalized analysis, the force contributions f_x, f_y and f_z are non-dimensionalized.

Dividing throughout by $\frac{1}{2}\rho V_a{}^2 c$ the non-dimensional form of the resultant force components are obtained as

$$C_{f_x} = C_l\left(\frac{-\sin\gamma}{g_b}\right) + C_d\left(\frac{J + \cos\theta\cos\gamma}{g_a}\right) \tag{7.a}$$

$$C_{f_y} = C_l\left(\frac{J\sin\theta\sin\gamma}{g_b}\right) + C_d\left(\frac{\sin\theta}{g_a}\right) \tag{7.b}$$

$$C_{f_z} = C_l\left(\frac{-\cos\gamma - J\cos\theta}{g_b}\right) + C_d\left(\frac{-\cos\theta\sin\gamma}{g_a}\right) \tag{7.c}$$

For easy interpretation and simplified analysis, the above coefficients are divided by the sectional drag coefficient to produce

$$\frac{C_{f_x}}{C_d} = \frac{C_l}{C_d}\left(\frac{-\sin\gamma}{g_b}\right) + \left(\frac{J + \cos\theta\cos\gamma}{g_a}\right) \tag{8.a}$$

$$\frac{C_{f_y}}{C_d} = \frac{C_l}{C_d}\left(\frac{J\sin\theta\sin\gamma}{g_b}\right) + \left(\frac{\sin\theta}{g_a}\right) \tag{8.b}$$

$$\frac{C_{f_z}}{C_d} = \frac{C_l}{C_d}\left(\frac{-\cos\gamma - J\cos\theta}{g_b}\right) + \left(\frac{-\cos\theta\sin\gamma}{g_a}\right) \tag{8.c}$$

C_{f_x}/C_d, C_{f_y}/C_d and C_{f_z}/C_d are the non-dimensionalized parameters corresponding to f_x, f_y and f_z, respectively. Hence, they will be used in further investigations to analyze the thrust, side force and lift contributions of the wing section to the vehicle.

3. Results and discussion

Observing equations (8.a to c), it can be noted that C_{f_x}/C_d, C_{f_y}/C_d and C_{f_z}/C_d are functions of the independent non-dimensional parameters C_l/C_d, J, θ and γ. In the following analysis, flapping amplitude, flapping speed and stroke plane orientation are optimized for various phases of flight.

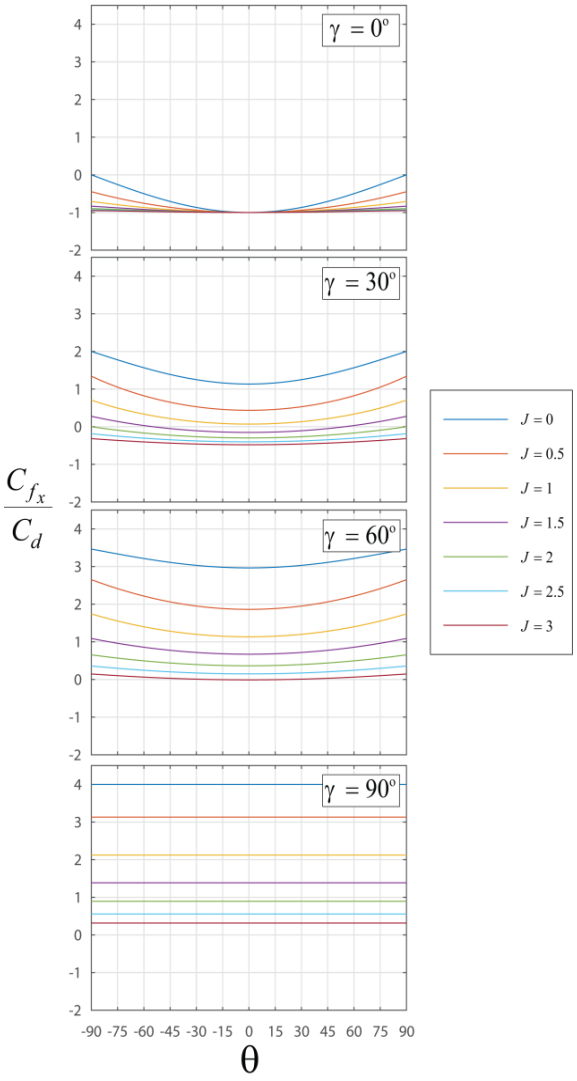

Figure 2. Plot of C_{f_x}/C_d vs. θ for various γ and J at $C_l/C_d = 4$.

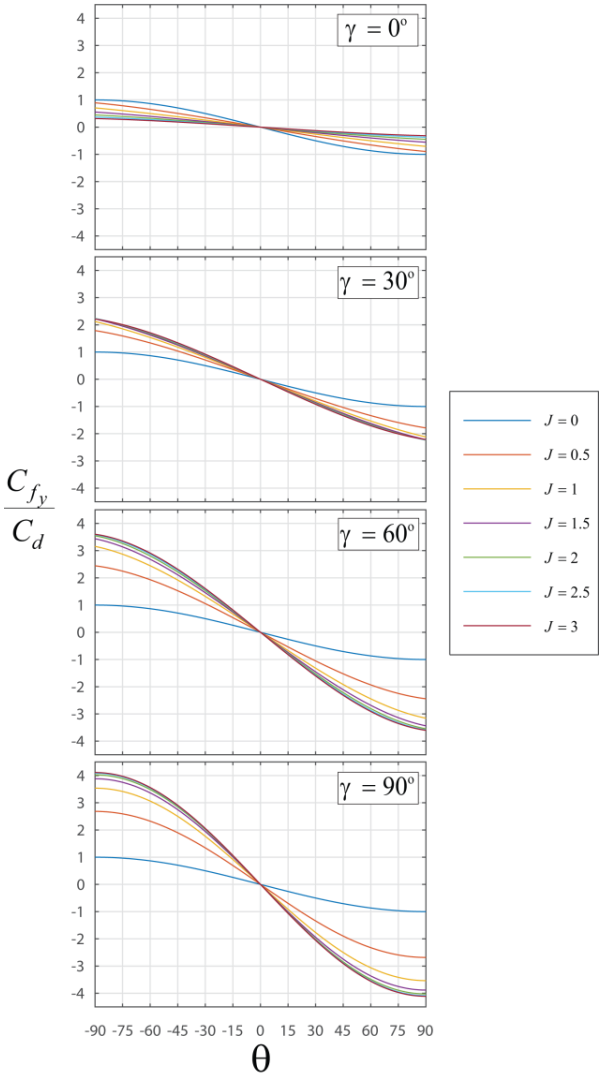

Figure 3. Plot of C_{f_y}/C_d vs. θ for various γ and J at $C_l/C_d = 4$.

In the normal symmetrical flapping conditions, the side force produced by the two wings will be cancelled by each other. Hence, this analysis focuses on maximizing thrust and lift production and minimizing the side force.

3.1. Optimization of Flapping Amplitude

C_{f_x}/C_d vary a little with θ and the value increases with J (figure 2). C_{f_z}/C_d varies considerably with θ and the variation increases with J (figure 4). Always C_{f_z}/C_d has its maximum value at the point where the wing crosses the flight frontal plane $(\theta = 0)$ and it reduces as the wing's position moves away from the frontal plane in both the directions (as $|\theta|$ increases from zero). C_{f_y}/C_d is zero when the wing's position crosses the flight frontal plane and it increases in magnitude as it moves away (figure 3). The magnitude also increases with J.

3.1.1. Takeoff and Hovering Phases. During takeoff and hovering phases, the wing can be flapped to the full range of θ, since C_{f_x}/C_d and C_{f_z}/C_d vary little and C_{f_y}/C_d has low magnitude at low J values. Hence, high flapping amplitude Λ is recommended.

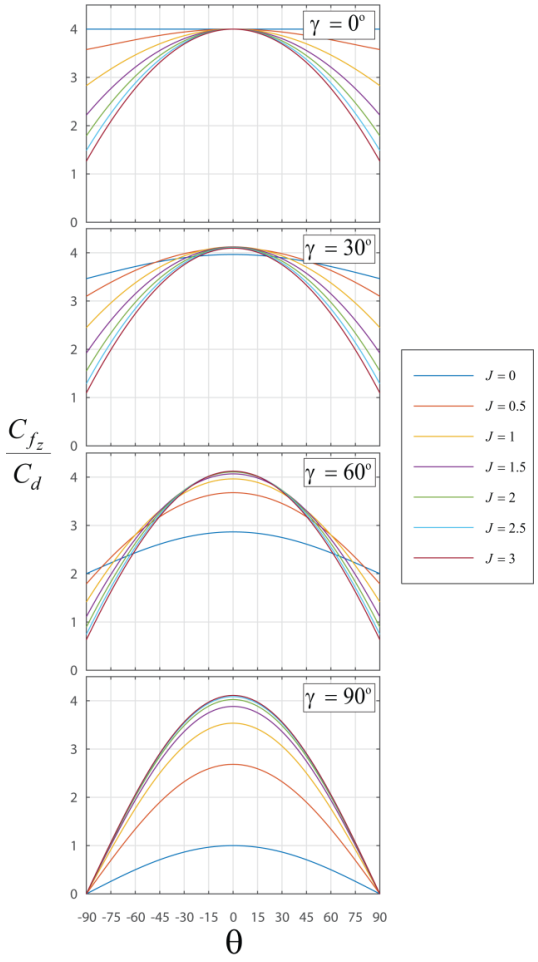

Figure 4. Plot of C_{f_z}/C_d vs. θ for various γ and J at $C_l/C_d = 4$.

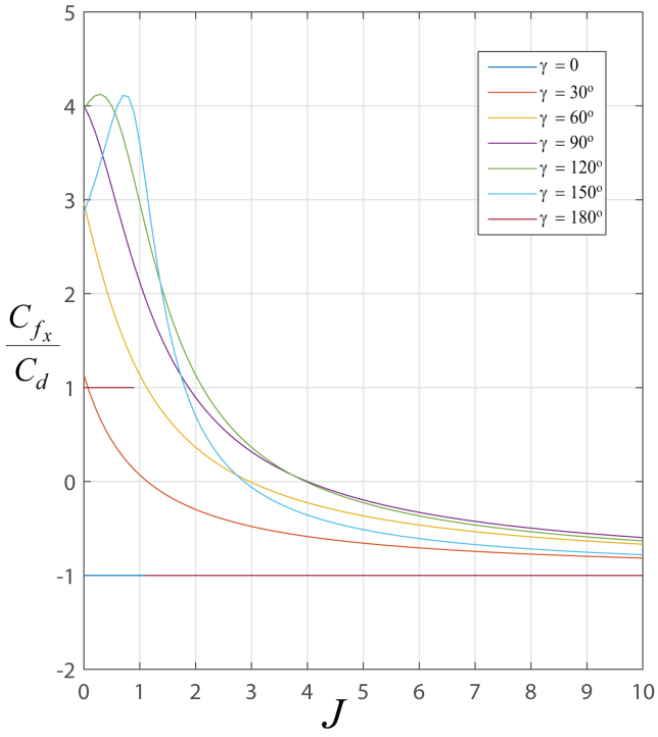

Figure. 5 Plot of C_{f_x}/C_d vs. J for various γ at $\theta = 0$ and $C_l/C_d = 4$.

3.1.2. Cruising and High Speed Flight Phases. As the flight velocity increases, the value of J increases. At high values of J, C_{f_y}/C_d has considerably higher values at higher values of θ. Moreover, C_{f_z}/C_d reduces as θ increases. Hence, the flapping amplitude Λ should be reduced (such that the wing's position does not move away much from the frontal plane).

3.2. Optimization of Stroke Plane Orientation

C_{f_x}/C_d increases with increase in γ and the variation reduces with J (figure 2 & 5). C_{f_z}/C_d reduces with increase in γ and the variation reduces with J (figure 4). C_{f_y}/C_d increases with increase in γ and the variation increases with J (figure 3).

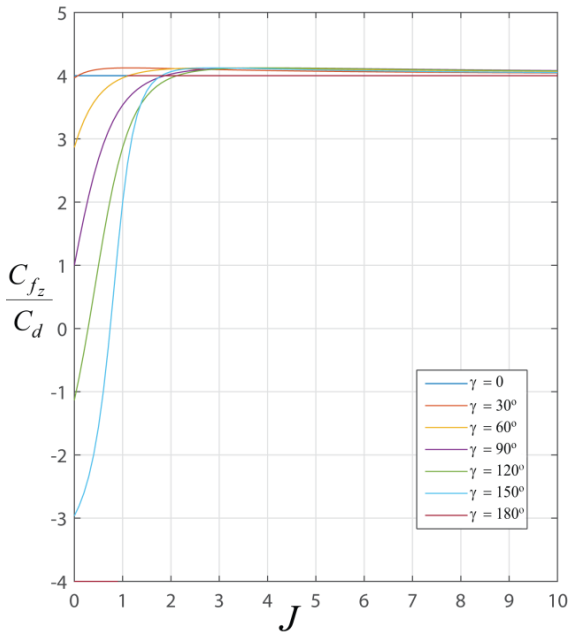

Figure 6. Plot of C_{f_z}/C_d vs. J for various γ at $\theta = 0$ and $C_l/C_d = 4$.

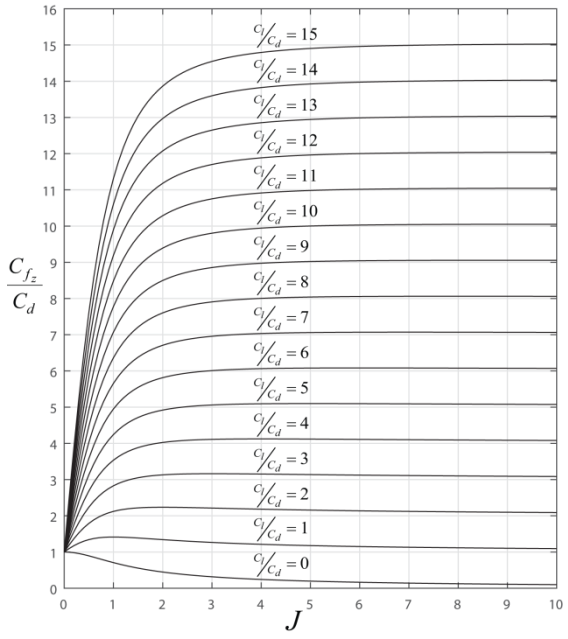

Figure 7. Plot of C_{f_z}/C_d vs J for various C_l/C_d at $\theta = 0$ and $\gamma = 90°$.

3.2.1. Takeoff and Hovering Phases. The primary requirement in these phases is to produce the necessary lift; either to liftoff the vehicle during takeoff or to sustain the flight position in air during hovering. C_{f_z}/C_d corresponding to low J reduces considerably with γ. Hence, during takeoff and hovering, a low value of γ should be maintained so that the sufficient amount of lift is produced.

3.2.2. Cruising and High Speed Flight Phases. C_{f_x}/C_d increases with increase in γ for a given value of J (figure 2 & 5). This demands that, for accelerating the flight or for flying at high speeds, the stroke plane orientation should be increased. However, increasing γ beyond 90° is not advisable. Because, there is only a little increase in thrust production (figure 5) besides having a huge reduction in lift production (figure 6). The problem of increase in the C_{f_y}/C_d resulting from the increase of γ can be solved by reducing the flapping amplitude as suggested in section 3.1.2.

3.3. Optimization of flapping speed

Equations (11.a to c) are not expressed directly in terms of the flapping speed. But, the property of flapping speed can be read by observing the property of the advance ratio J. Since J is defined by $J = -V_\infty/(r\dot{\theta})$, an increase J in corresponds to an increase in flight velocity V_∞ if the flapping speed $(-r\dot{\theta})$ is kept constant and a decrease in J corresponds to an increase in flapping speed $(-r\dot{\theta})$ if flight velocity V_∞ is kept constant.

Figure 5 shows a decrease in C_{f_x}/C_d with increase in J. Figure 6 shows a increase in C_{f_z}/C_d with increase in J. This seems to be a tradeoff. Yet, a careful study of various flight phases will help solving this.

3.3.1. Takeoff and hovering phases. In takeoff and hovering phases, V_∞ has very low magnitude. Therefore, the wing airfoil section depends more on the flapping speed to produce the aerodynamic forces. Also, lift production is the primary requirement and that alone can be considered for optimization in these phases.

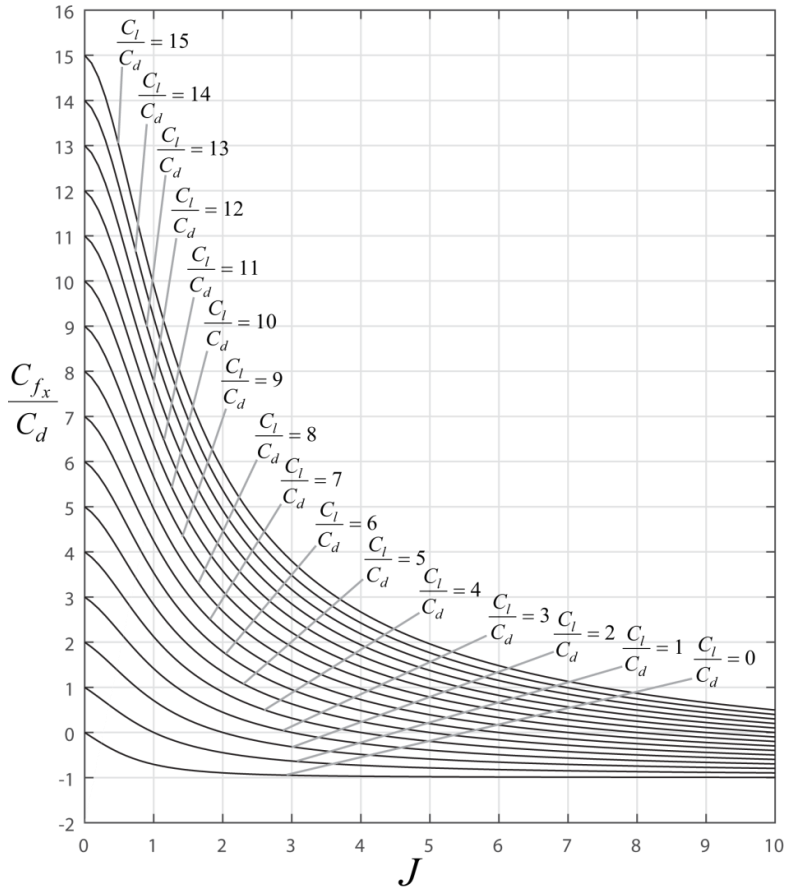

Figure 8. Plot of C_{f_x}/C_d vs. J for various C_l/C_d at $\theta = 0$ and $\gamma = 90°$.

The requirement of high flapping speed and availability of low flight velocity will reflect in very low value of J. Production of high lift in low J is possible by maintaining a low value of γ (figure 6). Also, by increasing C_l/C_d of the wing section, by maintaining an effective airfoil shape, will help increasing the lift production (figure 7).

3.3.2 Cruising and high-speed flight phases. In cruise and high speed flights the flight velocity is sufficient enough to produce the necessary lift by the wing. The work done by the wing is just to produce the necessary thrust to oppose the drag. Therefore, thrust production is the primary requirement of these phases.

An increase in flight velocity V_∞ will result in increase of J. As J increases C_{f_x}/C_d decreases and C_{f_z}/C_d increases (figure 5 & 6). This trade-off can be solved by increasing the C_l/C_d of the wing section by maintaining an effective airfoil shape (figure 7 & 8). If an acceleration to further high speed is desired, an increase in flapping speed and/or an increase in C_l/C_d should be done.

4. Conclusion

The contributions of the airfoil lift and drag to the vehicle's thrust, lift and side force, were found using vector mechanics and non-dimensionalized. Their variations with sectional lift to drag ratio, advance ratio, stroke plane orientation and instantaneous flapping angle are studied through a series of plots.

The symmetrical flapping condition was taken for analysis and the optimization was carried out with a performance objective to maximize lift and thrust production and to minimize side force. The findings from the analysis are as follows:

a) Takeoff needs high speed flapping at the highest possible stroke amplitude with a low stroke plane orientation with the flight frontal plane.
b) As the velocity increases, gradual increase of the stroke plane orientation combined with a reduction of the stroke amplitude and flapping speed will take to an optimized steady level flight.
c) Accelerating a steady flight can be done with an increase in stroke plane orientation and/or an increase in flapping speed and/or an increase in the lift to drag ratio produced by the wing section.
d) Flapping in hovering is similar to that of takeoff with minor adjustments in flapping speed and stroke plane orientation such that the position of the vehicle is sustained stationary.

The optimum values of flapping amplitude, flapping speed and stroke plane orientation at different flight phases are not produced quantitatively, rather qualitatively; so that to give a preliminary idea how to change the flapping style for different flight phases.

This research recommends for a wing, which could produce high lift to drag ratio in all phases of flight. Designing such a wing is the scope for further research, which will open a deep insight into the aerodynamic mechanism of flapping wings.

Discovery of optimized combinations of unsteady and quasi-steady force production techniques for different flight phases and analyzing them with proper aerodynamic tools will further fine-tune the optimized flapping styles. Experimental analyses based on this research will also disclose many new ideas in optimization of flapping flight.

5. References

[1] Hassanalian M, Abdelkefi A 2016 Effective design of flapping wing actuation mechanisms: theory and experiments *54th AIAA Aerospace Sciences Meeting* (Reston, Virginia: American Institute of Aeronautics and Astronautics)
[2] Nguyen T A, Vu Phan H, Au T K L and Park H C 2016 Experimental study on thrust and power of flapping-wing system based on rack-pinion mechanism. *Bioinspir. Biomim.* **11** 46001
[3] Hoff J, Ramezani A, Chung S-J and Hutchinson S Synergistic Design of a Bio-Inspired Micro Aerial Vehicle with Articulated Wings *Robotics: Science and Systems XII* (Robotics: Science and Systems Foundation)
[4] Yoon S, Kang L H and Jo S 2011 Development of Air Vehicle with Active Flapping and Twisting of Wing *J. Bionic Eng.* **8** 1–9
[5] Phan H V, Truong Q T, Au T K L and Park H C 2015 Effect of Wing Kinematics Modulation on Aerodynamic Force Generation in Hovering Insect-mimicking Flapping-wing Micro Air Vehicle *J. Bionic Eng.* **12** 539–554
[6] Wu G hao, Zeng L jiang and Ji L hong 2008 Measuring the Wing Kinematics of a Moth (Helicoverpa Armigera) by a Two-Dimensional Fringe Projection Method *J. Bionic Eng.* **5** 138–142
[7] Tobalske B W 2007 Biomechanics of bird flight. *J. Exp. Biol.* **210** 3135–3146
[8] Shyy W, Aono H, Chimakurthi S K, Trizila P, Kang C K, Cesnik C E S and Liu H 2010 Recent progress in flapping wing aerodynamics and aeroelasticity *Prog. Aerosp. Sci.* **46** 284–327
[9] Chin D D and Lentink D 2016 Flapping wing aerodynamics: from insects to vertebrates *J. Exp. Biol.* **219** 920–32
[10] Nguyen T T and Byun D 2008 Two-Dimensional Aerodynamic Models of Insect Flight for

Robotic Flapping Wing Mechanisms of Maximum Efficiency *J. Bionic Eng.* **5** 1–11
[11] Raman A, Allwyn K and Lijomon H M 2013 Quantified Aerodynamics for Flapping Wings *Trans. Control Mech. Syst.* **1** 48-56
[12] Taha H E, Hajj M R and Nayfeh A H 2012 Flight dynamics and control of flapping-wing MAVs: A review *Nonlinear Dyn.* **70** 907–39
[13] Taha H, Hajj M and Nayfeh A 2012 Optimization of wing kinematics for hovering MAVs using calculus of variation *14th AIAA/ISSMO Multidiscip.*
[14] BERMAN G J and WANG Z J 2007 Energy-minimizing kinematics in hovering insect flight *J. Fluid Mech.* **582** 153-168
[15] Anon Awesome Goose Takeoff In Slow Motion - YouTube
[16] Anon White Ibis White Bird Takes Flight Relaxation Video Slow Motion Casio EXILIM Pro EX-F1 at 300 fps - YouTube
[17] Anon Slo-Mo White pigeon flight - YouTube
[18] Anon Slow motion Birds in flight - YouTube
[19] Anon Scarlet Macaws take their medicine. Earthflight (Winged Planet) Narrator David Tennant) YouTube
[20] Brown R H J 1963 The Flight of Birds *Biol. Rev.* **38** 460–89
[21] Krashanitsa R Y, Silin D, Shkarayev S V and Abate G Flight Dynamics of a Flapping-Wing Air Vehicle
[22] Park J H and Yoon K-J 2008 Designing a Biomimetic Ornithopter Capable of Sustained and Controlled Flight *J. Bionic Eng.* **5** 39–47
[23] de Croon G C H E, Groen M A, De Wagter C, Remes B, Ruijsink R and van Oudheusden B W 2012 Design, aerodynamics and autonomy of the DelFly *Bioinspir. Biomim.* **7** 25003
[24] Brown R H J 1953 The flight of birds II. Wing function in relation to flight speed *J. Exp. Biol.* **30** 90–103
[25] Sachs G 2015 Aerodynamic Cost of Flapping *J. Bionic Eng.* **12** 61–9